

CHAPTER VI

ETHYLENE THIOUREA (ETU) AS CORROSION INHIBITOR FOR MILD STEEL IN 1N HYDROCHLORIC ACID

- 6.1 REVIEW OF LITERATURE
- 6.2 INHIBITOR MOLECULE
- 6.3 RESULTS AND DISCUSSION
- 6.4 CONCLUSIONS
- 6.5 REFERENCES

6.1 REVIEW OF LITERATURE

Mild steel is iron-carbon alloy containing less than 0.25 percent carbon which makes it more ductile and less hard thus rendering it unsuitable for structural work. Besides carbon, there are many metal elements that are a part of steel alloys. The elements other than iron and carbon, used in steel are chromium, manganese, tungsten and vanadium. All these elements along with carbon, act as hardening agents. That is, they prevent dislocations from occurring inside the iron crystals and prevent the lattice layers from sliding past each other. Varying the amounts of these hardening agents creates different grades of steel. The ductility, hardness and tensile strength are a function of the amount of carbon and other hardening agents, present in the alloy. The amount of carbon is a deciding factor, which decides hardness of the steel alloy. A steel alloy with a high carbon content is mild steel, which is in fact much harder and stronger than iron. Though, increased carbon content increases the hardness of the steel alloy, it causes a decrease in its ductility. Steel is very important in our day-to-day life, starting from the steel cook wares to scientific instruments like scalpel. Due to its cost-effectiveness and strength, steel is used in engineering works and in infrastructure developments such as roads, railways, bridges, buildings and stadiums. The ferromagnetic properties of mild steel make it ideal for manufacture of electrical devices and motors. Growth and development of the steel industry marks the economic progress of the country.

B.El Mehdi et al. conducted a comparative study of inhibitive effect of some new triazole derivatives(3,5-di(m-tolyl)-4-amino-1,2,4-triazole,3,5-di(m-tolyl)-4H-1,2,4-triazole) towards corrosion of mild steel in HCl solution using weight loss and electrochemical methods. Polarization studies reveal mixed type inhibition behavior and adsorption studies found that the inhibitors obey Langmuir adsorption isotherm model [1]. M.A Quraishi et al. also reported a new acid corrosion inhibitor for mild steel in 1N HCl using weight loss and polarization studies. Various kinetic and thermodynamic parameters (E_a , ΔG_{ads} , Q , ΔH , ΔS) were calculated and revealed that a strong interaction between inhibitor and mild steel surface. The negative value of

ΔG_{ads} indicates the spontaneous adsorption of inhibitor on the mild steel surface [2].

Hui- Long Wang et al. studied corrosion inhibition of mild steel in HCl solution by 4- salicylidane amino-3-phenyl-5-mercapto-1,2,4-triazole using weight loss and electrochemical techniques . Polarization studies showed that inhibitor is a mixed type one. Adsorption studies revealed chemisorption nature of the inhibitor. Surface analysis studies and thermodynamic calculations are also carried out [3]. M.A Quraishi and R Sardar studied the effect of some nitrogen and sulfur based synthetic inhibitors (5-mercapto-3-butyl-4-salicylidine imino-1,2,4-triazole, 5-mercapto-3-butyl-4-benzylidene imino-1,2,4-triazole, 5-mercapto-3-butyl-4-cinnamylidene imino-1,2,4-triazole) on mild steel in 1N HCl and 1N H₂SO₄ solutions using weight loss and potentiodynamic polarization studies. Adsorption of these compounds obey Temkins adsorption isotherm and polarization studies reveal that the inhibitors are mixed type in action [4].

Hui-Long Wang et al. studied inhibitive effect of some mercapto triazole derivatives on the corrosion of mild steel in 1M HCl medium using polarization and impedance studies. Polarization studies reveal the mixed type inhibition behavior of the molecule. Changes in impedance parameters are indicative of the adsorption of the compounds on the metal surface [5]. Kaan C Emregul et al. studied corrosion inhibition of steel with Schiff base compounds in 2M HCl using weight loss, polarization and impedance methods. The inhibitors function through Langmuir adsorption isotherm [6]. M. Bouklah et al. studied thiophene derivatives as inhibitors for corrosion of mild steel in 0.5 M H₂SO₄ by weight loss, electrochemical polarization and impedance measurements. Polarization reveals the cathodic type inhibition and adsorption gives an s-shaped adsorption isotherm [7]. M.S Morad reported the influence of cysteine and cystine on the corrosion behavior of mild steel in sulfide polluted sulphuric acid solution by using potentiodynamic polarization methods and a.c impedance techniques. The inhibitors act as anodic and obeys Temkin isotherm [8].

Hamdy H Hasssan investigated the inhibition of mild steel corrosion in HCl solution by Triazole derivatives (5-amino-1,2,4-triazole,5-amino-3-mercapto-1,2,4-triazole,5-amino-3-methylthio-1,2,4-triazole) by polarization and impedance methods. Time, temperature and thermodynamic treatments also done. These studies suggest chemisorption of the inhibitor molecule on the metal surface [9]. Ying Yan et al conduct electrochemical and quantum chemical study of purines as corrosion inhibitor for mild steel in 1M HCl. Polarization studies reveal mixed type behavior of the inhibitor and quantum chemical calculations confirm the adsorption mechanism of the molecule [10]. R.Solmaz et al. conducted adsorption and corrosion inhibition properties of 2-amino-5- mercapto -1, 3, 4-thiadiazole on mild steel in hydrochloric acid media using polarization and impedance studies [11]. Emel Bayol et al. studied interaction of some schiff base compounds with mild steel surface in hydrochloric acid solution using impedance and polarization studies [12].

M. Ehteshamzadeh et al. reported two new schiff base compounds (N,N' -ortho-phenylenacetyl acetone imine and 4- [(3 -{ [1- (2- hydroxyl phenyl) methylidene] amino} propyl] ethanemidol]- 1,3- benzenediol) on inhibition performance in 1 M HCl solution by electroscopic impedance studies. Both of them obey Langmuir adsorption isotherm [13]. S.V Ramesh and V.Adhikari studied that N'-(4-diethylamino) benzylidene]-3- {[8-(trifluoromethyl)quinolin-4-yl]thio} propane hydrazide) as an effective inhibitor for mild steel corrosion in acid media [HCl (1M,2M),H₂SO₄ (0.5M ,1M)] using weight loss, EIS and polarization methods. Inhibition efficiency in different acid media are found to be 0.5M H₂SO₄>1M HCl>2M HCl>1M H₂SO₄. Inhibition assumed to occur via adsorption and molecule act as anodic inhibitor. Thermodynamic parameters were calculated and chemisorption mechanism is proposed [14]. A.K Singh and M.A Quraishi studied the effect of some bis-thiadiazole derivatives on the corrosion of mild steel in HCl using weight loss, electrochemical polarization and impedance measurements. Thermodynamic and activation parameters were calculated. At lower concentration of the inhibitor physisorption is observed and at higher concentrations chemisorption was favored. They also conducted inhibition

effect of diethylcarbamide on the corrosion of mild steel in HCl using weight loss, electrochemical polarization, impedance measurements and atomic force microscopy techniques. Results show that inhibition occurs through adsorption on the metal surface without modifying the mechanism of corrosion process. Polarization studies suggest that molecule is a mixed type inhibitor, predominantly controls the cathodic reaction. Activation parameters (E_a , ΔH , ΔS) and thermodynamic parameters (ΔG_{ads} , ΔH_{ads} , ΔS_{ads}) were calculated to investigate the mechanism of the inhibition process [15-16].

P.Lowmunkhong, D.Ungtharak and P.Sutthivaiyakit studied tryptamine as a corrosion inhibitor for mild steel in HCl solution using linear polarization, potentiodynamic polarization and EIS techniques. The inhibition efficiency increases with increase in concentration of the inhibitor. Polarization studies reveal mixed type behavior of the inhibitor molecule. The molecule follow Langmuir adsorption isotherm model [17].

M.A Amin, K.F Khaled and S.A Fadl-Alah tested the validity of Tafel extrapolation method for monitoring corrosion of mild steel in HCl solution by experimental and theoretical studies using glycine and its derivatives. Polarization studies show that the inhibitor behaves as mixed type. Electrochemical Frequency modulation (EFM) and inductively coupled Plasma atomic emission spectroscopy (ICP-AES) were conducted to monitor the corrosion rate and the results are comparable with those recorded using Tafel extrapolation method. Density functional theory is used to study the structural properties of the inhibitor molecule and protection efficiency of these compounds is showed a certain relationship to HOMO energy, Mulliken atomic charges and Fukui indices [18].

I.B Obot and N.O Obi-Egbedi conducted an experimental and theoretical investigation on the adsorption properties and inhibition of mild steel corrosion in H_2SO_4 by ketoconazole. Adsorption follows Langmuir isotherm with negative value of G_{ads} suggesting a stable and spontaneous inhibition process. Quantum chemical approach was used to calculate some electronic properties of the molecule in order to ascertain any correlation between inhibition effect and molecular structure [19]. I.Ahamad, R.Prasad and M.A

Quraishi conducted studies on adsorption and inhibitive properties of some new mannich bases of isatin derivatives on corrosion of mild steel in 1M HCl using weight loss, polarization studies, and EIS and quantum chemical calculation methods. The value of activation energy and various thermodynamic parameters were calculated. Polarization studies showed that the inhibitors are mixed type. Adsorption process obeys Langmuir adsorption isotherm. They also conducted thermodynamic, electrochemical and quantum chemical investigation of some Schiff bases as corrosion inhibitors for mild steel in HCl solution. Activation energy and other thermodynamic parameters were calculated to explain the mechanism of corrosion inhibition. The adsorption follow Langmuir adsorption isotherm model. Polarization studies indicate mixed type behavior. The computed chemical properties viz E_a , E_{MBG} show good correlation with experimental inhibition efficiency [20-21].

A.Y Musa et al. studied inhibition of mild steel corrosion in 2.5M H_2SO_4 by 4-amino-5-phenyl-4H-1,2,4-triazole-3-thiol at different temperatures using open circuit potential, potentiodynamic and impedance measurements. Inhibition efficiency increased with the inhibitor concentration but decreased with temperature. The kinetics and thermodynamic parameters were calculated and propose chemisorption mechanism [22]. Y.Tang, X.Yang, W.Yang, Y.Chen and R.Wan conducted experimental and molecular dynamics studies on corrosion behavior of mild steel in 1M HCl by 2-amino-5-phenyl-1,3,4-thiadiazole (APT) using potentiodynamic polarization and EIS techniques. Adsorption of APT molecule obeys Langmuir adsorption isotherm. The molecular dynamics method has been used to simulate the adsorption of ATP molecule and solvent on the iron surface [23].

N.O Obi-Egbedi and I.B. Obot investigated inhibition properties, thermodynamic and quantum chemical studies of alloxazine on mild steel corrosion in H_2SO_4 using weight loss and computational techniques. Adsorption follow Temkin model. Both activation and thermodynamic parameters were calculated. Adsorption follows first order kinetics. DFT studies explain the mechanism of inhibitor action [24]. F. Bentiss et al. studied the relationship between corrosion inhibiting effect and molecular

structure of 2, 5-bis (n-pyridyl) - 1,3,4-thiadiazole derivatives in acidic media (1M HCl, 0.5 M H₂SO₄ & 1M HClO₄) using a.c impedance and DFT studies. Calculated values of free energy reveal chemisorption nature of the compound. Quantum chemical calculation and experimental inhibitive efficiency were correlated and indicates that the inhibition effect is explained in terms of electronic properties [25].

6.2 INHIBITOR MOLECULE

The inhibitor Ethylene thiourea (ETU) was procured from E.Merck and the structure is given Fig.6.1.The percentage compositions of various elements present in the inhibitor molecule obtained by elemental analysis using CHN Analyser (Model Elemental Vario EL III) at CUSAT, Kochi and compared with the (theoretical) values. C: 35.06(35.27), H: 5.61(5.92), N: 29.87(27.42) and S: 30.90(31.39).The medium used throughout the experiment is 1N HCl.

6.3 RESULTS AND DISCUSSION

6.3.1 Potentiodynamic polarization measurements

The potentiodynamic polarization studies were conducted in the potential range of -250 mV to +250 mV with a sweep rate of 1000 mV/minutes (16 mV/sec).Polarization curve of the mild steel in 1N HCl with out and with various concentration of ETU (25, 50, 75 &100 ppm) at 303,313 & 323 K are shown in Fig.6.2 (a,b & c). It can be seen that both cathodic and anodic reactions of mild steel were inhibited by increase in the concentration of ETU at all the studied temperatures. It is clear that both cathodic and anodic curves show a lower current density in the presence of the inhibitor than those recorded in the additive free solutions indicating the mixed type behavior of the inhibitor.

The Electrochemical corrosion parameters like corrosion potential (E_{corr}), cathodic and anodic Tafel slopes (β_c and β_a) and corrosion current density (i_{corr}) obtained from Tafel extrapolation of the polarization curve are given in Table V1.1. The inhibitor molecule first adsorb on the mild steel surface and blocking the available reaction sites [26]. The surface coverage increases with

the inhibitor concentration. The presence of defects on the metal surface permits free access to H⁺ ions [27] and a significant dissolution of metal takes place, followed by desorption of inhibition film from the metal surface [28]. The formation of surface inhibitor film on the mild steel surface provides considerable protection to the metal against corrosion. This film reduces the active surface area exposed to the corrosive medium and delays the hydrogen evolution and iron dissolution [29-30].

6.3.2 Linear Polarization studies

In order to determine the polarization resistance, R_p, the potential of the working electrode was ramped ±10mV in the vicinity of the corrosion potential at a scan rate of 1000mV/min. Polarization resistance were determined from the slope of the potential versus current lines,

$$R_p = A \frac{dE}{di} \text{ where } A \text{ is the surface area of the electrode.}$$

The percentage inhibition efficiency is evaluated as follows:

$$IE \% = \frac{R_p^o - R_p}{R_p^o} \times 100, \text{ } R_p^o \text{ and } R_p \text{ are the polarization resistance values in}$$

the absence and presence of the inhibitor respectively.

The R_p values increases with increasing inhibitor concentration as seen in Fig.6.3 (a, b & c). The rest potential values were used to calculate the inhibition efficiency. The parallel increase in the corrosion inhibition efficiency for mild steel in 1 N HCl with increasing inhibitor concentration may be due to the adsorption of inhibitor molecule on metal surface.

6.3.3 Electrochemical impedance spectroscopy

Electrochemical Impedance Spectroscopy (EIS) provides a rapid and convenient way to evaluate the performance of the organic-coated metals and has been widely used for the investigation of protective properties of organic inhibitors on metals. It does not disturb the double layer at the metal/solution interface [31-32]. Therefore, more reliable results can be obtained from this

technique. Electrochemical impedance spectroscopy (EIS) measurements were carried out in the frequency range 10 KHz to 10Hz with amplitude of 10 mV (RMS) using a.c signals at open circuit potential. The Nyquist plots, the representative Bode diagrams and impedance plots for the uninhibited 1 N HCl and solution containing different inhibitor concentrations at various temperatures are given in Fig.6.4(a-c), 5(a-c) & 6(a-c).The Nyquist diagrams show single capacitive loop, with increasing diameter with concentration of the inhibitor, attributed to charge transfer of the corrosion process. It is evident from Fig.6.4 (a, b & c) that the impedance loops measured are depressed semi-circles with their centers below the real axis due to the roughness and other in-homogeneities of the electrode surface [33-35]. So one constant phase element (Q) is substituted for the capacitive element in the equation to get a more accurate fit. The impedance of a constant phase element is described by the expression:

$$Z_Q = Y_0^{-1} (j\omega)^{-n}$$

where Y_0 is a proportional factor, n has the meaning of a phase shift. For $n = 0$, Q represents a resistance; for $n = 1$, a capacitance; for $n = 0.5$, a Warburg element and for $n = -1$ an inductance. According to Hsu and Mansfeld [36], the values of the double layer capacitance (C_{dl}) can be obtained from the equation:

$$C_{dl} = Y_0(\omega_m'')^{n-1}$$

where ω_m'' is the frequency at which the imaginary part of the impedance has a maximum.

Charge transfer resistance (R_{ct}) and double layer capacitance (C_{dl}) were given in Table V1.2. It is observed from Table V1.2 that the values of the polarization resistance increases with the increase in inhibitor concentration, due to the corrosion protection effect of the inhibitor molecules. The inhibition efficiencies calculated from EIS studies, show the same trend of polarization measurements. The difference of inhibition efficiency of these two methods may be attributed to the different surface status of the electrode

in these two measurements. EIS measurements were performed at the rest potential, while in polarization measurements the electrode surface was polarized due to high overpotential, non-uniform current distributions resulted from cell geometry, solution conductivity, counter and reference electrode placement etc. and will lead to the difference between the electrode area actually undergoing polarization and the total area [37]. As it can be seen from Table VI.2, the C_{dl} values tend to decrease with the increase of the inhibitor concentration. The decrease in the C_{dl} , which can result from a decrease in local dielectric constant and/or an increase in the thickness of the electrical double layer, suggests that ETU molecule functions by adsorption at the metal/solution interface [38].

6.3.4 Effect of Temperature

The effect of temperature on various corrosion parameters E_{corr} , I_{corr} and IE was studied in 1N HCl at temperature range 303,313 & 323 K in the absence and presence of different concentrations of inhibitor. Variation of temperature has almost no effect on the general shape of the polarization curves. The results were listed in Table VI.1. An inspection of above table shows that, as the temperature increase, the values of I_{corr} increases and inhibition efficiency and surface coverage decreases. This proves that the inhibition occurs through the adsorption of the additives on the metal surface. Desorption is aided by an increase in temperature. The activation parameters for the corrosion process were calculated from Arrhenius- type plot according to the following equation

$$I_{corr} = k \exp\left(-\frac{E_a}{RT}\right) \quad (1)$$

where E_a is the activation energy, k is the frequency factor, T is the absolute temperature, and R is the gas constant. Values of apparent activation energies of corrosion (E_a) for mild steel in 1N HCl without and with various concentration of ETU determined from the slope of $\ln(I_{corr})$ versus $1/T$ plot (Fig.6.7) are shown in Table VI.3. Inspection of the data shows that the activation energy is lower in the presence of inhibitors than in its absence. The decrease of E_a value with ETU concentration (Table VI.3) is typical of physisorption. This was attributed to slow rate of inhibitor adsorption at

higher temperature, as reported by Hoar and Holiday [39]. Bur, Riggs and Hurd [40] explained that the decrease in the activation energy of corrosion at higher levels of inhibition arises from a shift of the net corrosion reaction from that on the uncovered part on the metal surface to the covered one.

An alternative formulation of Arrhenius equation is

$$I_{\text{corr}} = \frac{RT}{Nh} \exp\left(\frac{\Delta S_a^\circ}{R}\right) \exp\left(-\frac{\Delta H_a^\circ}{RT}\right) \quad (2)$$

where h is plank's constant, N is Avogadro's number ΔS_a° is the entropy of activation and ΔH_a° is the enthalpy of activation. A plot of $\ln(I_{\text{corr}}/T)$ against $1/T$ gave a straight line with a slope of $(-\Delta H_a^\circ/R)$ and an intercept $(\ln R/Nh + \Delta S_a^\circ/R)$ from which the values of ΔH_a° and ΔS_a° were calculated (Fig.6.8). The positive signs of the enthalpies (ΔH_a°) reflect the endothermic nature of steel dissolution process. Large and negative values of entropies (ΔS_a°) imply that the activated complex in the rate determining steps represents association rather than dissociation step, meaning that a decrease in disordering takes place on going from reactant to the activated complex [41].

6.3.5 Adsorption Studies

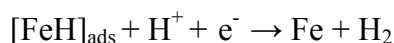
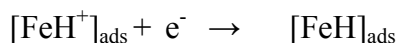
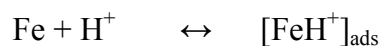
From attempts to fit the θ values to different isotherms, the best-fit result obtained with the Langmuir isotherm. The plot of C_{inh}/θ against C_{inh} of ETU in 1 N HCl gives a straight line as shown in Fig.6.9.

The free energy of adsorption ΔG_{ads} is calculated using the relation,

$$\Delta G_{\text{ads}} = -RT \ln \left[\frac{55.5\theta}{C(1-\theta)} \right] \quad (3)$$

where C is the concentration of the inhibitor expressed in ppm. The negative value of ΔG_{ads} ensures the spontaneity of adsorption process and stability of the adsorbed layer on the mild steel surface. Generally the value ΔG_{ads} around -20kJ mol^{-1} or lower are consistent with physisorption, while those around -40kJ mol^{-1} or higher value involve chemisorptions [42]. The values of

ΔG_{ads} for ETU are given in Table V1.4 and these values indicate that the molecule is physisorbed. The hetero atoms of the inhibitor molecule make it adsorbed readily on the metal surface forming an insoluble stable film on the metal surface and thus decreasing metal dissolution. The probable mechanism of the cathodic hydrogen evolution reaction may be given as



The protonated ETU molecule are adsorbed at cathodic sites in competition with hydrogen ions that going to reduce H_2 gas evolution

6.4 CONCLUSIONS

- The inhibitor molecule show high inhibitive efficiency for mild steel in 1N HCl.
- The percentage inhibition efficiency increases with concentration and decreases with exposure time and temperature.
- The degree of surface coverage increases with inhibitor concentrations.
- Polarization studies reveal that ETU act as mixed type inhibitor.
- The inhibitor molecules adsorb on the mild steel surface and blocking the reaction sites. The surface area available for the attack of the corrosive species decreases with increasing inhibitor concentrations and temperature.

6.5 REFERENCES

1. Mehdi.B.El, Mernari.B, Traisnel.M, Bentiss.F & Lagrenee.M, *Mater. Chem. phy.* 77 (2002) 489.
2. Quraishi.M.A, Ishtique.Ahamed, Ashish Kumar Singh, Sudhish kumar shukla, B.Lal & Vakail.Singh, *Mater. Chem. phy.* 112 (2002) 1035.
3. Hui- Long.Wang, Hong-BoFan & Jia-Shen Zheng, *Mater. Chem. Phys.* 77 (2002) 65.
4. Quraishi.M.A & Sardar.R, *Indian Journal Of Chemical Technology.* 11 (2004) 103.
5. Hui-Long Wang, Rui-Bin Liu & Jian Xin, *Corros .Sci.*46 (2004) 2455.
6. Kaan C Emregul, A. Abdulkadir Akay & Orhan Alakol, *Mater. Chem. and Phy.* 93 (2005) 325.
7. Bouklah.M, Hammouti.B, Benkaddour.M & Benhadda.T, *J. Appl. Electrochem.* 35 (2005) 1095.
8. Morad.M.S, *J Appli Electrochem.* 37 (2007) 1191.
9. Hamdy H. Hassan, *Electrochim acta* .53 (2007) 1722.
10. Ying Yan, Weihue Li, Lankun Cai & Baorong Hou, *Electrochemica Acta.* 53 (2008) 5953.
11. Solmaz.R, Kardas.G, Yazici.B & Erbil.M, *Colloids & surfaces A:* 312 (2008) 7.
12. Emel.Bayol, Tijen.Gurten, Ali Gurten.A & Erbil.M *Mater. Chem. Phys.* 112 (2008) 624.
13. Ehteshamzadeh.M, Jafari.A.H. Esmael.Naderi & Hosseini.M.G. *Mater. Chem. Phy.* 113 (2009) 986.
14. Ramesh.S.V & Adhikari.V, *Mater. Chem .Phys.* 115 (2009) 618.
15. Singh.A.K & Quraishi.M.A, *Corros sci.* 52 (2010) 1373.

16. Singh.A.K & Quraishi.M.A, *Corros. sci.* 52 (2010) 1529.
17. Lowmunkhong.P, Ungtharak.D & Sutthivaiyakit.P, *Corros. sci.* 52 (2010) 3.
18. Amin.M.A, Khaled.K.F & Fadi-Alah S.A, *Corros Sci.* 52 (2010) 140.
19. Obot.I.B & Obi-Egbedi.N.O, *Corros. Sci.* 52 (2010) 198.
20. Ahamad .I , Prasad.R & Quraishi.M.A, *Corros. Sci.* 52 (2010) 1472.
21. Ahamad.I , Prasad.R & Quraishi M.A, *Corros .Sci.* 52 (2010) 433.
22. Musa.A.Y *Corros.Sci* 52 (2010) 526.
23. Tang.Y. Yang X, Yang.W. Chen.Y& Wan.R, *Corros Sci.* 52 (2010) 242.
24. Obi-Egbedi .N.O & Obot .I.B ,*Corros. Sci.* 53 (2011) 263.
25. Bentiss F, Mernari B, Traisnel M,Vezin H & Lagrenee.M, *Corros. Sci.* 53 (2011) 487.
26. Fuchs-Godec .R, *Colloids Surf. A: Physicochem.Eng.Aspects* 280 (2006) 130.
27. Chetouani .A, Hammouti .B, Benhadda. T& Daoudi .M, *Appl. Surf. Sci.* 249 (2005) 375.
28. El .Mehdi B, Mernari .B, Traisnel .M, Bentiss .F& Lagrenee .M, *Mater. Chem. Phys.*77 (2002) 489.
29. El Achouri .M, Kertit. S, Goultaya. H .M, Nciri .B, Bensouda .Y, Perez. L,Infante .M .R & Elkacemi .K, *Prog. Org. Coat.* 43 (2001) 267.
30. Lorenz .W .J & Mansfeld .F, *Corros. Sci.* 31 (1986) 467.
31. Erbil. M, *Chim. Acta Turcica* 1 (1988) 59.

32. Dehri .I, H.So˘zu˘ sag˘lam & Erbil. M., *Prog. Org. Coat.* 48 (2003) 118.
33. Mansfeld . F, *Corrosion.* 37 (1981) 301.
34. Mac Cafferty .E, *Corros. Sci.* 39 (1997) 243.
35. Morad .M.S , *Corros. Sci.* 42 (2000) 1313.
36. Hsu .C.H, & Mansfeld F , *Corrosion.* 57 (2001) 747.
37. Kelly.R.G, Scully.J.R,Shoesmith,D.W & Buchheit R.G, *Electrochemical Techniques in Corrosion Science and Engineering, Marcel Dekker, Inc. New York* .148 (2002).
38. Lebrini .M, Lagrenee. M, Traisnel. M, Gengembre. L, Vezin. H & Bentiss. F , *Appl. Surf. Sci.* 253 (2007) 9267.
39. Hoar. T .P.D & Hollyday .R .D, *J.Appl.Chem.*3 (1953) 502.
40. Riggs .L .O & Hurd .T. I, *Corrosion.* 23 (1967) 252.
41. Marsh. J, *Advanced Organic Chemistry, third edn, Wiley Eastern, New Delhi*, (1988).
42. Yurt.A, Bereket .G, Kivrak .A, Balaban .A & Erk .B, *J.Appl.Electrochem.* 35 (2005) 1025.

Table VI.1 Electrochemical parameters of mild Steel with Ethylene thiourea (ETU) in 1N HCl at 303,313 & 323 K

Temp. (K)	Conc. (ppm)	- E _{corr} (mV)	L.P.R (Ω cm ²)	β _a (mVdec ⁻¹)	β _c (mV dec ⁻¹)	I _{corr} (μA cm ⁻²)	C.R (mm/yr)	I.E (%)
303	Blank	473	45	88	89	425	0.5723	----
	25	472	54	65	90	263	0.2240	38
	50	481	68	65	74	179	0.0840	57
	75	493	86	64	79	139	0.0710	67
	100	501	94	72	50	88	0.0640	79
313	Blank	483	30	104	136	1130	4.97	----
	25	500	32	92	126	734	3.32	35
	50	508	35	100	123	509	2.42	55
	75	513	37	97	105	407	1.07	64
	100	516	41	106	89	271	0.81	76
323	Blank	511	17	102	144	1460	6.24	----
	25	498	18	92	131	964	4.29	34
	50	506	20	95	126	686	3.17	53
	75	513	22	98	106	554	2.49	62
	100	514	24	104	89	380	2.07	74

Table VI.2 AC Impedance data of mild Steel in 1N HCl at 303,313 & 323 K

Temp. (K)	Conc. (ppm)	Rct ($\Omega \text{ cm}^2$)	Cdl ($\mu\text{F cm}^{-2}$)	Icorr ($\mu\text{A cm}^{-2}$)	n	C.R (mm/yr)	I.E (%)
303	Blank	305	132	85	0.80	0.9984	----
	25	478	57	56	0.82	0.6537	36
	50	683	49	38	0.84	0.4423	55
	75	881	48	29	0.85	0.3432	65
	100	1223	45	21	0.91	0.2472	75
313	Blank	65	150	397	0.78	4.622	----
	25	98	95	242	0.81	2.807	34
	50	142	94	175	0.83	2.032	54
	75	179	65	139	0.85	1.613	63
	100	247	56	105	0.87	1.220	73
323	Blank	37	181	593	0.76	6.902	----
	25	54	146	408	0.82	4.710	32
	50	77	129	337	0.80	3.923	53
	75	94	111	285	0.82	3.312	59
	100	121	94	214	0.83	2.474	69

Table VI.3 The value of activation parameters, E_a , ΔH_a^0 , ΔS_a^0 for mild steel in 1N HCl in the absence presence of different concentrations of ETU

Conc. (ppm)	E_a (kJmol^{-1})	ΔH_a^0 (kJmol^{-1})	$-\Delta S_a^0$ ($\text{Jmol}^{-1}\text{K}^{-1}$)	R^2
Blank	1.34	1.42	182.74	0.94
25	1.28	1.35	186.15	0.94
50	1.24	1.29	189.23	0.95
75	1.20	1.26	190.89	0.95
100	1.14	1.19	194.01	0.94

Table VI.4 Adsorption parameters of inhibitor (ETU) for corrosion of mild steel in 1N HCl

Tem(K)	$\Delta G_{\text{ads}}(\text{kJ mol}^{-1})$ & $K_{\text{ads}}(\text{mol}^{-1})$							
	Inhibitor Conc: (ppm)							
	25		50		75		100	
303	-6.411	2296	-6.619	2078	-6.649	2526	-7.135	3060
313	-6.393	2103	-6.733	2301	-6.646	2527	-7.100	2759
323	-6.355	1920	-6.840	2040	-6.406	2418	-6.805	3061

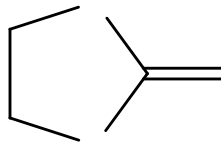


Fig .6.1 Structure of Ethylene thiourea (ETU)

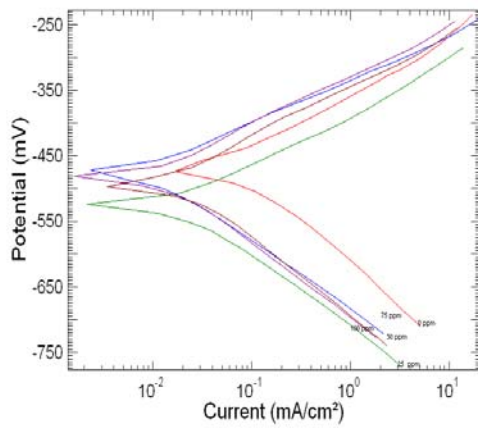


Fig.6.2a

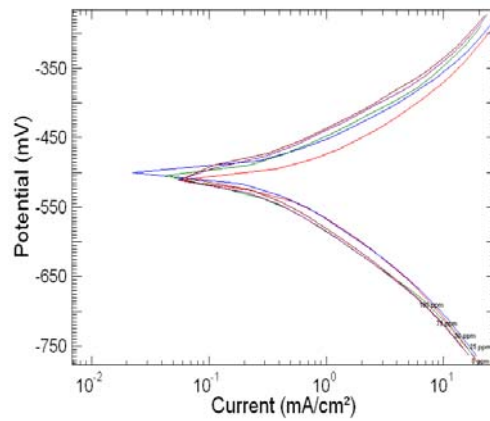


Fig.6.2b

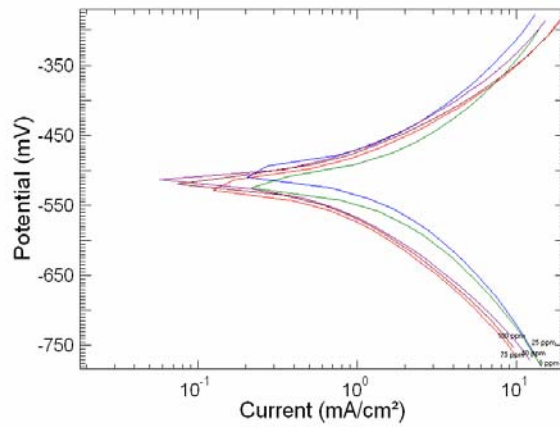


Fig.6.2c

Fig.6.2 Polarization curve for mild steel in 1N HCl in the presence and absence of various concentrations of ETU at a) 303, b) 313 & c) 323 K

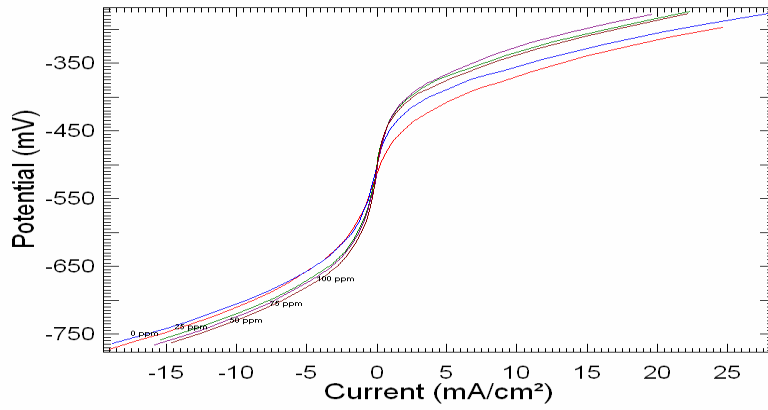


Fig.6. 3a

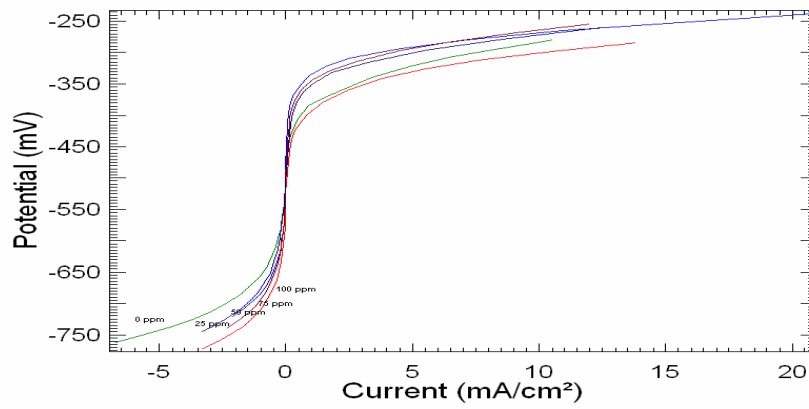


Fig.6. 3 b

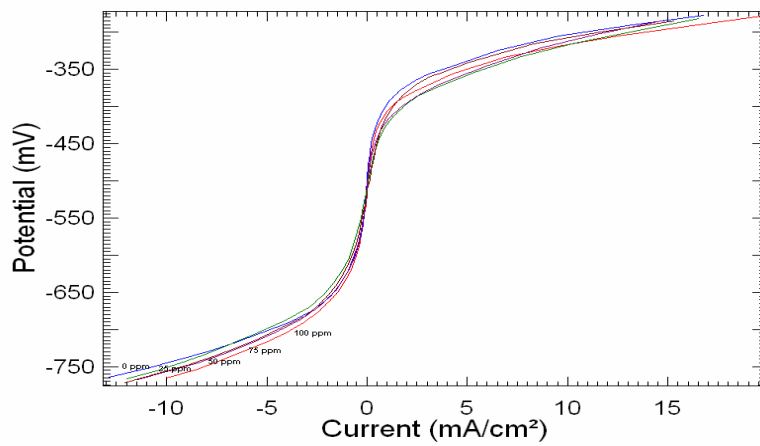


Fig.6.3 c

Fig 6.3 LPR plot for mild steel in 1N HCl in the presence and absence of various concentrations of ETU at a) 303, b) 313 & c) 323 K

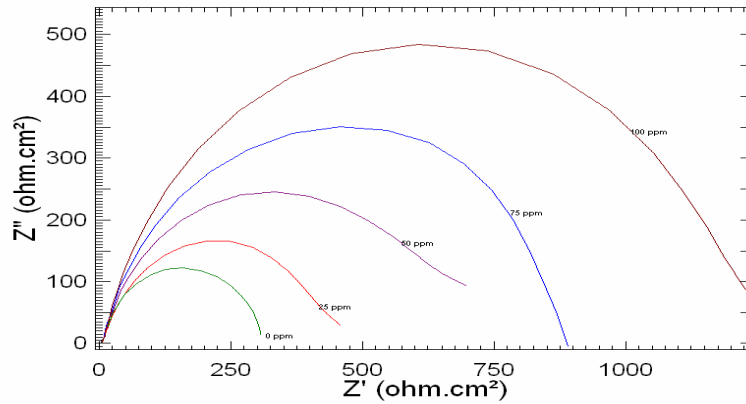


Fig.6.4a

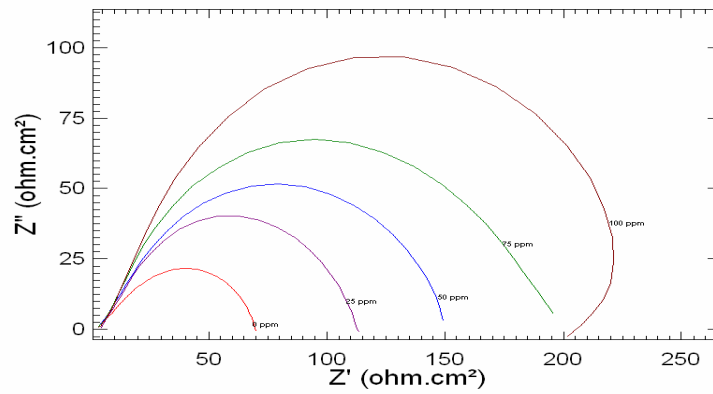


Fig .6.4b

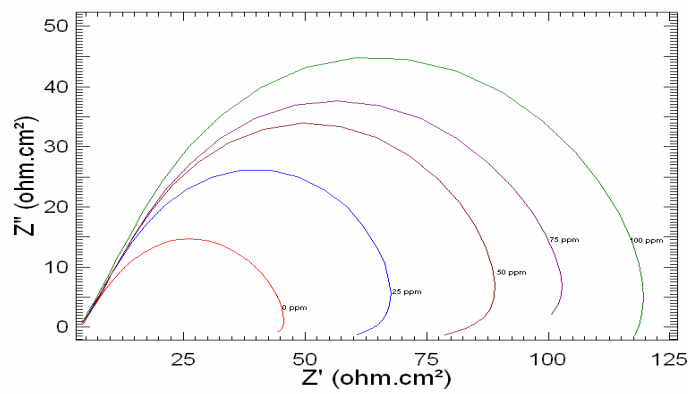


Fig .6.4c

Fig.6.4 Nyquist plot for mild steel in 1N HCl in the presence and absence of various concentrations of ETU at a) 303, b) 313 & c) 323 K

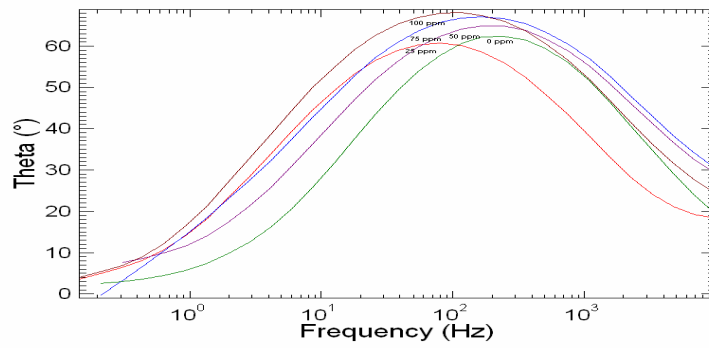


Fig .6.5a

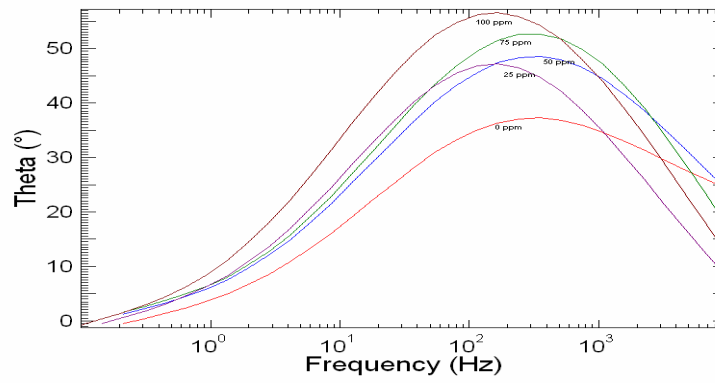


Fig. 6.5b

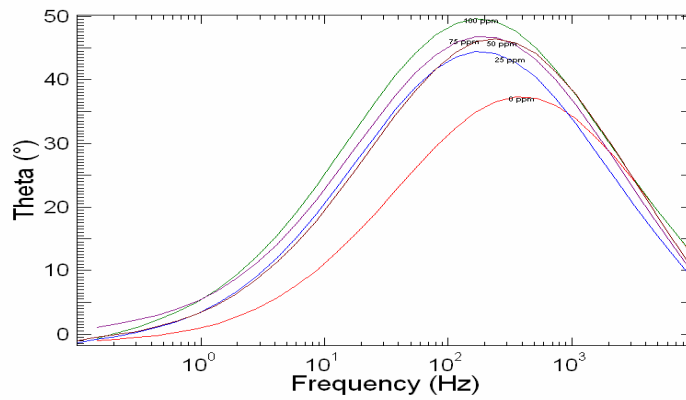


Fig. 6.5c

Fig.6.5 Bode-phase plots of mild steel in 1N HCl at a) 303, b) 313 & c) 323 K

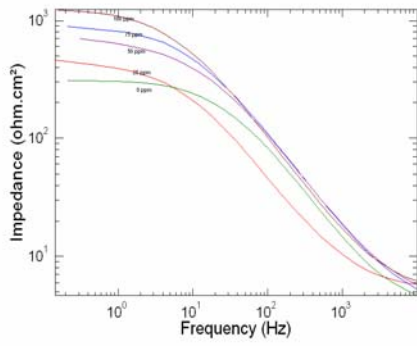


Fig .6.6a

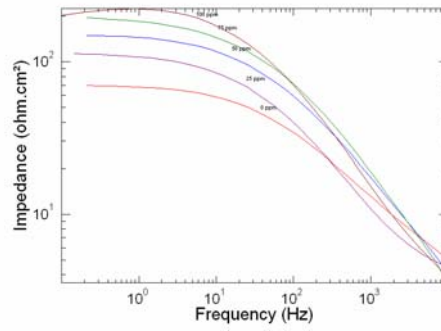


Fig .6.6b

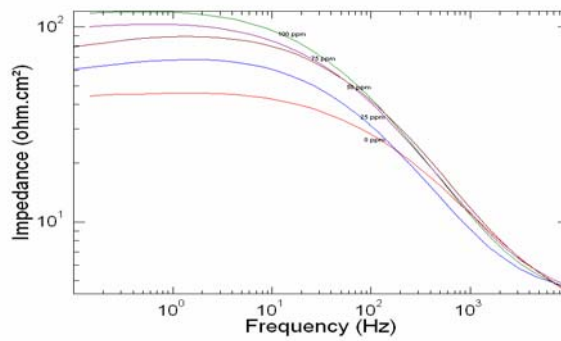


Fig .6. 6c

Fig .6.6 Impedance plot for mild steel in 1N HCl in the presence and absence of various concentrations of ETU at a) 303, b)313 & c) 323 K

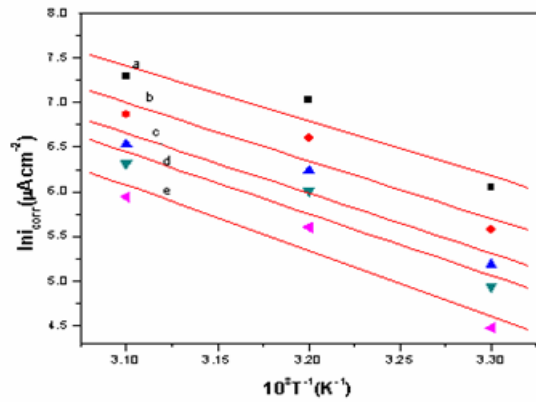


Fig .6.7 Arrhenius plots of $\ln(I_{corr})$ versus $1/T$ at different concentrations of ETU: a: blank b: 25 ppm c: 50 ppm d: 75ppm e: 100 ppm.

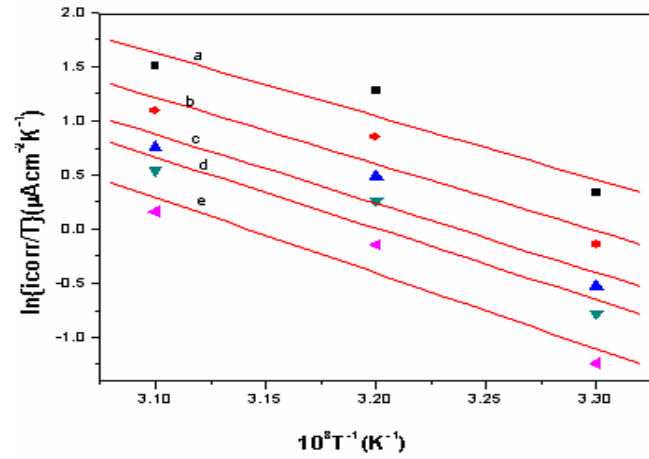


Fig .6.8 Arrhenius plots of $\ln(I_{corr})/T$ versus $1/T$ at different concentrations of ETU a: blank b: 25 ppm c: 50 ppm d: 75ppm e: 100 ppm

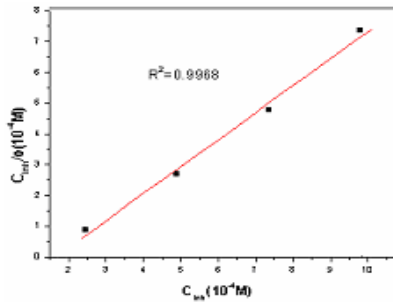


Fig .6.9a

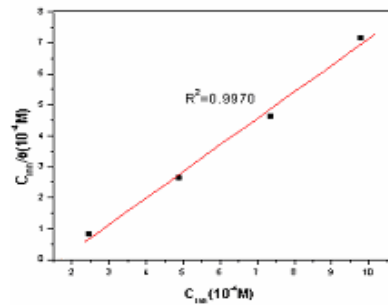


Fig .6. 9b

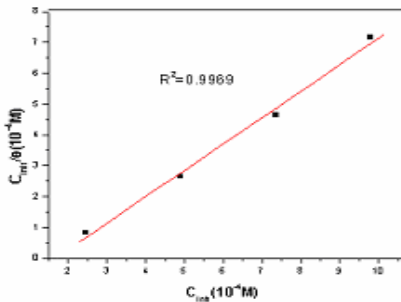


Fig .6.9c

Fig 6.9. Langmuir adsorption isotherm for mild steel in 1N HCl in the absence and presence of ETU at a) 303, b) 313 & c) 323 K